Cell Reports

Report

The Emergence of the Spatial Structure of Tectal Spontaneous Activity Is Independent of Visual Inputs

Graphical Abstract

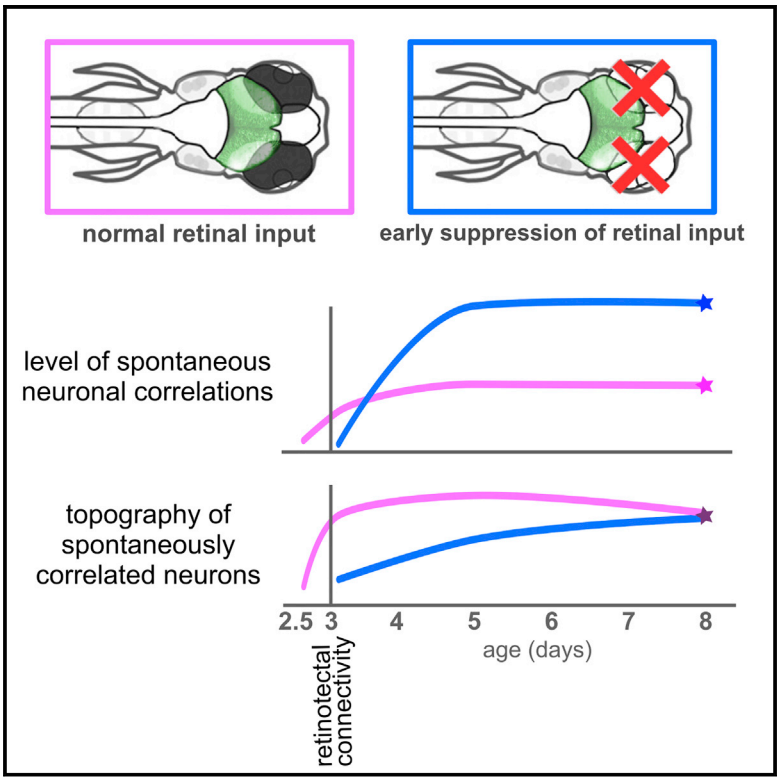

Authors

Thomas Pietri, Sebastián A. Romano, Verónica Pérez-Schuster, Jonathan Boulanger-Weill, Virginie Candat, Germán Sumbre

Correspondence

sumbre@biologie.ens.fr

In Brief

The influence of retinal inputs on the development of the spontaneous neuronal activity of the tectal circuit is unknown. Pietri et al. show that retinal inputs are dispensable for the development of the spatial structure of spontaneous tectal activity, suggesting that the tectal circuit is preconfigured for its functional role.

Highlights

- Development of tectal circuitry is influenced by the onset of retinal inputs
- Enucleations impact the development of the tectum's spontaneous activity correlations
- Enucleations only delay the topography of the correlated activity
- In the absence of retinal inputs, the tectal circuitry is capable of predicting behavior

Pietri et al., 2017, Cell Reports *19*, 939–948
May 2, 2017
http://dx.doi.org/10.1016/j.celrep.2017.04.015

CellPress

Cell Reports
Report

The Emergence of the Spatial Structure of Tectal Spontaneous Activity Is Independent of Visual Inputs

Thomas Pietri,[1,2] Sebastián A. Romano,[1,3] Verónica Pérez-Schuster,[1,4] Jonathan Boulanger-Weill,[1] Virginie Candat,[1] and Germán Sumbre[1,5,*]

[1]IBENS, Département de Biologie, Ecole Normale Supérieure, CNRS, Inserm, PSL Research University, 75005 Paris, France
[2]Present address: Biological Sciences, New Jersey Institute of Technology, Newark, NJ 07102, USA
[3]Present address: Instituto de Investigación en Biomedicina de Buenos Aires (IBioBA) – CONICET – Partner Institute of the Max Planck Society, Buenos Aires C1425FQD, Argentina
[4]Present address: Laboratorio de Neurobiología de la Memoria, Departamento Fisiología, Biología Molecular y Celular and Departamento de Física, UBA, Buenos Aires C1428EG, Argentina
[5]Lead Contact
*Correspondence: sumbre@biologie.ens.fr
http://dx.doi.org/10.1016/j.celrep.2017.04.015

SUMMARY

The brain is spontaneously active, even in the absence of sensory stimulation. The functionally mature zebrafish optic tectum shows spontaneous activity patterns reflecting a functional connectivity adapted for the circuit's functional role and predictive of behavior. However, neither the emergence of these patterns during development nor the role of retinal inputs in their maturation has been characterized. Using two-photon calcium imaging, we analyzed spontaneous activity in intact and enucleated zebrafish larvae throughout tectum development. At the onset of retinotectal connections, intact larvae showed major changes in the spatiotemporal structure of spontaneous activity. Although the absence of retinal inputs had a significant impact on the development of the temporal structure, the tectum was still capable of developing a spatial structure associated with the circuit's functional roles and predictive of behavior. We conclude that neither visual experience nor intrinsic retinal activity is essential for the emergence of a spatially structured functional circuit.

INTRODUCTION

Sensory brain areas are continuously active, even in the absence of external stimulation. This ongoing spontaneous activity, defined as the intrinsic brain activity not driven by sensory stimuli, was once considered to be independent biophysical noise and thought to interfere with brain computations (Faisal et al., 2008; Tolhurst et al., 1983). This view has changed in recent years, as spontaneous activity has been found to be structured in space and time (Fiser et al., 2004; Jetti et al., 2014; Kenet et al., 2003; Kirkby et al., 2013; Romano et al., 2015; Smith and Kohn, 2008). In sensory brain areas, spontaneous activity can exhibit spatial patterns that match functional sensory maps (Jetti et al., 2014; Kenet et al., 2003; Romano et al., 2015).

Across the different sensory modalities, the visual system is the most extensively investigated. Although the initial organization of the retinorecipient brain areas is coarsely established by molecular cues (Triplett, 2014), activity-dependent mechanisms are thought to be essential for their maturation (Huberman et al., 2008). In the developing optic tectum, visual conditioning can alter neuronal functional properties, such as the formation of neuronal receptive fields (Vislay-Meltzer et al., 2006; Zhou et al., 2003) and the development of intratectal connectivity (Pratt et al., 2008). Furthermore, it causes short-term changes in spontaneous circuit dynamics (Sumbre et al., 2008). On the other hand, impeding visual experience by dark-rearing zebrafish larvae hardly alters their visual tectal response properties (Niell and Smith, 2005). Yet, in the tectum of dark-reared *Xenopus* tadpoles, temporal correlations between neurons and the reliability of their responses to a visual stimulus are significantly reduced (Xu et al., 2011). Besides visual experience, the retinorecipient circuits can also be influenced by the intrinsic activity of the retina (Ackman and Crair, 2014). Several studies have shown the crucial role of intrinsic retinal activity on the proper organization of retinal ganglion cell (RGC) projections within their target circuits (formation of retinotopic and eye-segregation maps; Kirkby et al., 2013; Kita et al., 2015). However, only a few have examined the effect of the retina on the maturation of the spontaneous activity of retinorecipient circuits. Specifically, optic nerve transection, or disruption of retinal waves (in the β2-nAChR mouse knockout) before eye opening, induced an increase of the spontaneous activity in the dorsal lateral geniculate nucleus of ferrets (Weliky and Katz, 1999) and in the superior colliculus (SC) of mice (Burbridge et al., 2014).

Despite these advances, a comprehensive study on the development of the spontaneous activity of retinorecipient areas, and on the influence of retinal activity on this process, is still lacking. To that end, we examined the single-neuron and circuit developmental dynamics of the spontaneous activity of the optic tectum

of intact, non-anesthetized, non-paralyzed, behaving zebrafish larvae throughout the main period of its functional maturation. These results were then compared to those from enucleated larvae whose tecta never received retinal inputs.

The optic tectum of the zebrafish, homologous to the mammalian SC, is involved in spatial vision detection (e.g., detection of prey) and generation of orienting motor commands (Gahtan et al., 2005; Krauzlis et al., 2013). In the functionally mature tectal circuit, ongoing spontaneous activity is organized in assemblies composed of highly correlated neurons. These neuronal assemblies are spatially organized reflecting the functional retinotopic map, they are tuned to biologically relevant visual stimuli (e.g., prey), and their activation predicted orienting tail movements. This suggests that the tectal circuitry is adapted for its functional role (Romano et al., 2015).

In the present study, we observed that the development of the spatiotemporal structure of spontaneous activity markedly changed at the onset of retinotectal connections, at 3 days post-fertilization (dpf; Niell and Smith, 2005; Stuermer, 1988). In retina-deprived conditions, the development of a spatiotemporal structure was delayed. By 8 dpf, when the tectal circuitry is functionally mature (Niell and Smith, 2005; Romano et al., 2015), the temporal structure (correlation level of neuronal activities) remained strongly impacted by retinal-input deprivation, yet the spatial structure (the topography of neuronal assemblies) reached similar values to those of intact larvae. Moreover, the deprived tectal circuit appeared functional, as the spontaneous activation of its tectal assemblies was still predictive of self-generated motor behaviors.

RESULTS

Development of Tectal Neurons' Spontaneous Activity

To study the maturation of the intrinsic network dynamics of the optic tectum, we monitored the spontaneous activity of transgenic zebrafish larvae expressing pan-neuronally the genetically encoded calcium indicator GCaMP3 (Tian et al., 2009), using two-photon scanning microscopy. This technique enables monitoring of the spontaneous dynamics of a significant portion of the optic tectum (893 ± 14 neurons from 135 larvae) at different developmental stages, in the presence (66–70, 74–80, 122–128, and 193–199 hr post-fertilization, hereinafter referred to in the text as 2.5, 3, 5, and 8 dpf) or absence (3, 5, and 8 dpf) of the main tectal sensory input, the retinal afferents (Figure 1A).

We first examined different properties of single tectal neurons: the average frequency of the Ca^{2+} transients (Figure 1B), their duration (Figure 1C), and their amplitude (ΔF/F; Figure 1D). In intact 2.5-dpf larvae, 7.63% ± 2.27% of the neurons did not show significant Ca^{2+} transients during the 1-hr recording period (silent neurons). At all other developmental stages, less than 0.22% ± 0.07% of the neurons were silent. The average frequency of neuronal Ca^{2+} events showed a progressive increase during development of the intact larvae (Figure 1B). In contrast, between 2.5 and 3 dpf, the period at which the retina establishes a functional connection with the optic tectum (functional synaptic connectivity; Niell and Smith, 2005), abrupt changes occurred in the duration (decrease from 2.5 to 3 dpf, $p = 5.10^{-4}$; Figure 1C) and the amplitude (increase, $p < 10^{-4}$; Figure 1D) of the Ca^{2+} events. The developmental dynamics of the frequency, duration, and amplitude of the Ca^{2+} events were remarkably different in larvae enucleated at 2 dpf (before the retina creates functional connections with the optic tectum). Their frequency sharply increased at 8 dpf (0.054 Hz versus 0.015 Hz in intact 8-dpf larvae; $p < 10^{-4}$). In contrast, their duration at 3 and 5 dpf remained similar to that of 2.5-dpf intact larvae ($p > 0.39$ and $p > 0.61$, respectively) but decreased to a level similar to that of intact larvae by 8 dpf ($p > 0.27$). Throughout maturation, we observed a constant increase in the frequency of spontaneous synchronous Ca^{2+} events (synchronous events were defined as periods in which at least 10% of the imaged tectal neurons were active at a given imaged frame). In enucleated larvae, this increase was significantly larger than in intact ones. Although the frequency of synchronous events at 3 dpf was not significantly different from that of intact larvae at 2.5 dpf ($p > 0.66$), we observed a large increase at 5 and 8 dpf ($p < 10^{-4}$; Figure 1E).

Overall, these results suggest that, at the onset of retinotectal interactions, the new excitatory retinal inputs strongly influence the maturation of the tectal neurons, while their absence creates a long-lasting profound plasticity effect (Keck et al., 2013). The differences in the duration and the amplitude of the spontaneous Ca^{2+}-events caused by the enucleations suggest that retinal inputs play an important role in the early physiological maturation of the tectal neurons (Sheroziya et al., 2009; Warp et al., 2012). In addition, the development of large synchronous events in the course of tectal maturation also suggests that the spontaneous tectal activity is temporally structured.

Development of Spontaneous Activity Neuronal Pairwise Correlations

To evaluate the putative temporal structure of the spontaneous activity in the optic tectum and its development, we first computed the neuron pairwise spontaneous activity Pearson's correlation coefficients at each developmental stage in intact and enucleated larvae (Figures S1A and S1B). Since we observed dramatically different levels of overall activity in the different conditions, we assessed the significance of these correlations by computing the Jensen-Shannon distance (JSD) between the distributions of correlations found in the measured and time-shuffled calcium activities (Figure 1F; JSD is a measurement of the difference between two distributions: here, it increases with the significance of the measured correlations). In intact animals, the average JSD progressively increased from stage to stage across development. In contrast, enucleated larvae showed a significantly larger average JSD value at 5 dpf than at 3 dpf ($p < 10^{-5}$); the latter was closer to the average JSD of 2.5-dpf intact larvae than to that of 3-dpf intact larvae. In addition, this temporal structure mostly reflected correlations within each tectal hemisphere in both intact and enucleated larvae (Figures S1C and S1D). However, a few high-correlation values were also observed between neuronal pairs across tectal hemispheres, reflecting the existence of specific functional connections between both hemispheres, either directly through the intertectal commissure or indirectly via other relay nuclei (Nevin et al., 2010). The lack of retinal inputs equally affected the development of intra- and intertectal correlations. Since the retina only projects to the contralateral tectum (Burrill and Easter, 1994), the

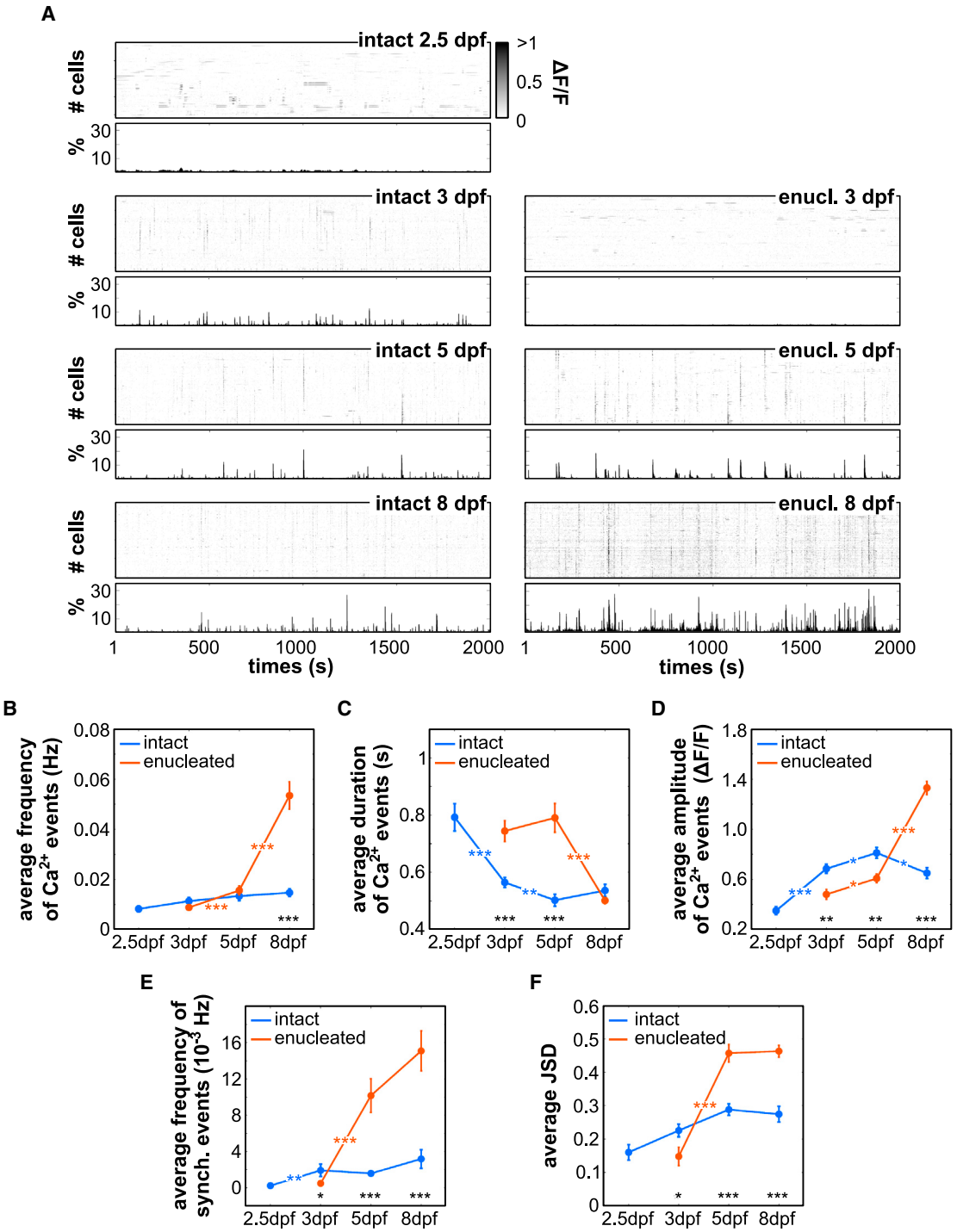

Figure 1. Maturation of the Spontaneous Tectal Activity in Intact and Retinal Input Deprived Larvae

(A) Raster plot examples of the spontaneous significant Ca^{2+} events of intact larvae at 2.5, 3, 5, and 8 dpf (left column, ns = 880, 1,012, 927 and 810 neurons, respectively) and an enucleated larva at 3, 5, and 8 dpf (right column, ns = 980, 882, and 879 neurons, respectively). The rasters represent a period of 2,000 s out of ~1 hr of recording sessions. Gray scale: amplitude of the Ca^{2+} events. The percentage of active neurons at each time point is represented below each raster plot.

(B–D) Developmental dynamics of the average frequency (B), duration (C), and relative fluorescence variation (D; ΔF/F) of the spontaneous Ca^{2+} events.

(E) Average frequency of the synchronous spontaneous Ca^{2+} events.

(F) Average distance between the distributions of the pairwise correlation coefficients and their respective random surrogate versions for each developmental stage in intact and enucleated larvae, quantified as JSD. Blue indicates intact larvae, and red indicates enucleated larvae.

*: $p < 0.05$; **: $p < 0.01$; ***: $p < 0.001$. Error bars indicate SEM.

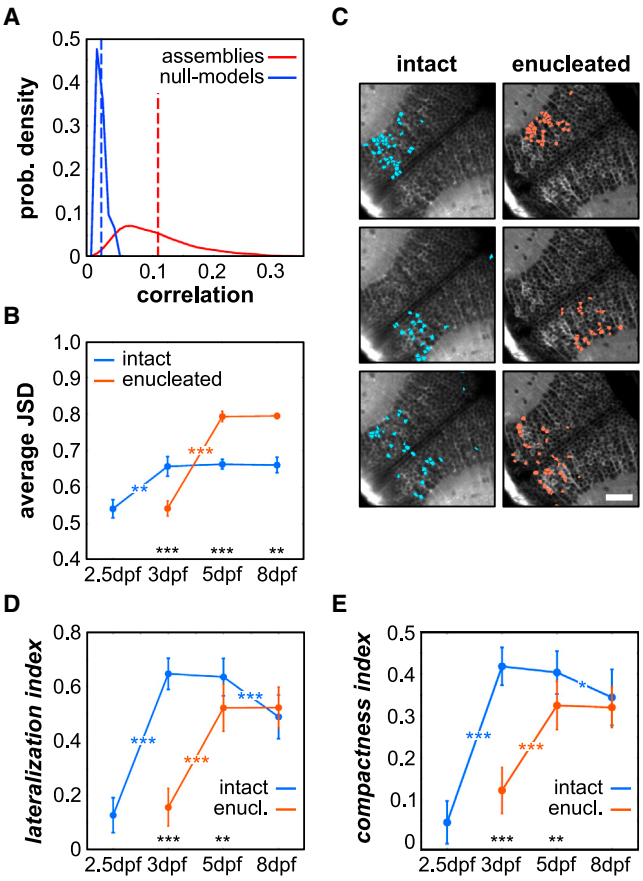

Figure 2. The Tectal Spontaneous Activity Structure Is Organized in Functional Neuronal Assemblies

(A) Probability (prob.) density of the distributions of the average correlations between neurons within each assembly and the corresponding null model, in intact larvae 5 dpf. The dotted lines represent the average correlation, in red for the data (0.108 ± 0.010) and blue for the null models (0.016 ± 0.002).

(B) Average JSD for the spontaneous neuronal assemblies across the different developmental stages, in intact and enucleated conditions.

(C) Topographies of representative neuronal assemblies emerging from the spontaneous activity of a 5 dpf intact and enucleated larva. Scale bar, 100 μm.

(D and E) Average index of lateralization, depicting the position of neurons within an assembly across both tecta (D), and index of compactness, representing the dispersion of neurons within a given assembly (E), for the neuronal assemblies during development, in intact and enucleated (enucl.) larvae.

Blue indicates intact larvae, and red indicates enucleated larvae in (B), (D), and (E).

*: $p < 0.05$; **: $p < 0.01$; ***: $p < 0.001$. Error bars indicate SEM.

latter observation indicates that common retinal inputs alone cannot explain the observed developmental changes. Overall, these results suggest an important strengthening of the overall connectivity in the tectal network after the formation of retinotectal connections.

Spontaneous Tectal Activity Is Organized into Neuronal Assemblies, even in the Absence of Retinal Inputs

Having demonstrated the establishment of significant temporal correlations among tectal neurons, we then asked whether these correlated neurons displayed a specific topographic organization (spatial structure). For this purpose, we used a recently developed method based on dimensionality reduction (principal-component analysis) and factor analysis for data clustering, which allowed the extraction of neuronal assemblies composed of highly correlated neurons while allowing for overlap between the neuronal assemblies (so that neurons could belong to different assemblies at different time points; Figures 2A and 2B). The number of assemblies, as well as the number of neurons per assembly, largely evolved during development (Figures S2A and S2B). While the average number of assemblies in enucleated larvae was mostly smaller across developmental stages when compared to intact larvae, they showed similar developmental dynamics (Figure S2A). The average number of neurons per neuronal assembly of enucleated larvae reached the same level as that of intact ones by 8 dpf ($p = 0.34$; Figure S2B).

To assess the significance of different temporal and spatial characteristics of these neuronal assemblies, we generated control null models by shuffling the identity of the neurons composing each assembly. This procedure randomized the topographies of the assemblies while keeping intact the number of neurons per assembly and the topographic position and activity time series of each neuron. Since the level of correlations between pairs of neurons may depend on the frequency of Ca^{2+} events, we chose the null-model assemblies with an average activity similar to that of their respective spontaneous assemblies (within 1 SD). We then normalized the respective values of the temporal and spatial traits of the different assemblies with respect to their corresponding null models.

Consistent with the observation that the majority of the high-correlation coefficients were between neurons belonging to the same tectal hemisphere, the spontaneous neuronal assemblies showed topographies that were often within the boundaries of a single tectal hemisphere (Figure 2C). However, during development, the assemblies presented large differences in terms of topographic dispersion of their neurons. We defined two indexes to assess the evolution of their topography: a *lateralization index* to quantify the distribution of each assembly with respect to both tectal hemispheres (Figure 2D) and a *compactness index* proportional to the topographical density of the neurons within each assembly (Figure 2E). In intact larvae, lateralization and compactness indexes significantly increased upon the arrival of retinal inputs to the tectum at 3 dpf ($p < 10^{-4}$ for both indexes), reaching a plateau at 5 dpf. A slight decrease was observed at 8 dpf ($p < 0.002$ for the lateralization index, and $p = 0.017$ for the compactness index, from 5 to 8 dpf). Noticeably, at 2.5 dpf, the assemblies already tended to be localized within one hemisphere (lateralization index significantly higher than 0; $p < 10^{-3}$). Enucleated larvae showed similar, although delayed, developmental dynamics. At 3 dpf, the average value of lateralization and compactness indexes did not significantly differ from that of 2.5-dpf intact larvae ($p > 0.85$), but they reached values similar to those of intact larvae at 8 dpf ($p > 0.19$ for the lateralization index, and $p > 0.57$ for the compactness index).

Since the spontaneous neuronal assemblies revealed coherent activity of their constitutive neurons, we defined a *matching index* (MI) for each assembly to evaluate their activation dynamics (Figure S2C). The MI was based on the similarity

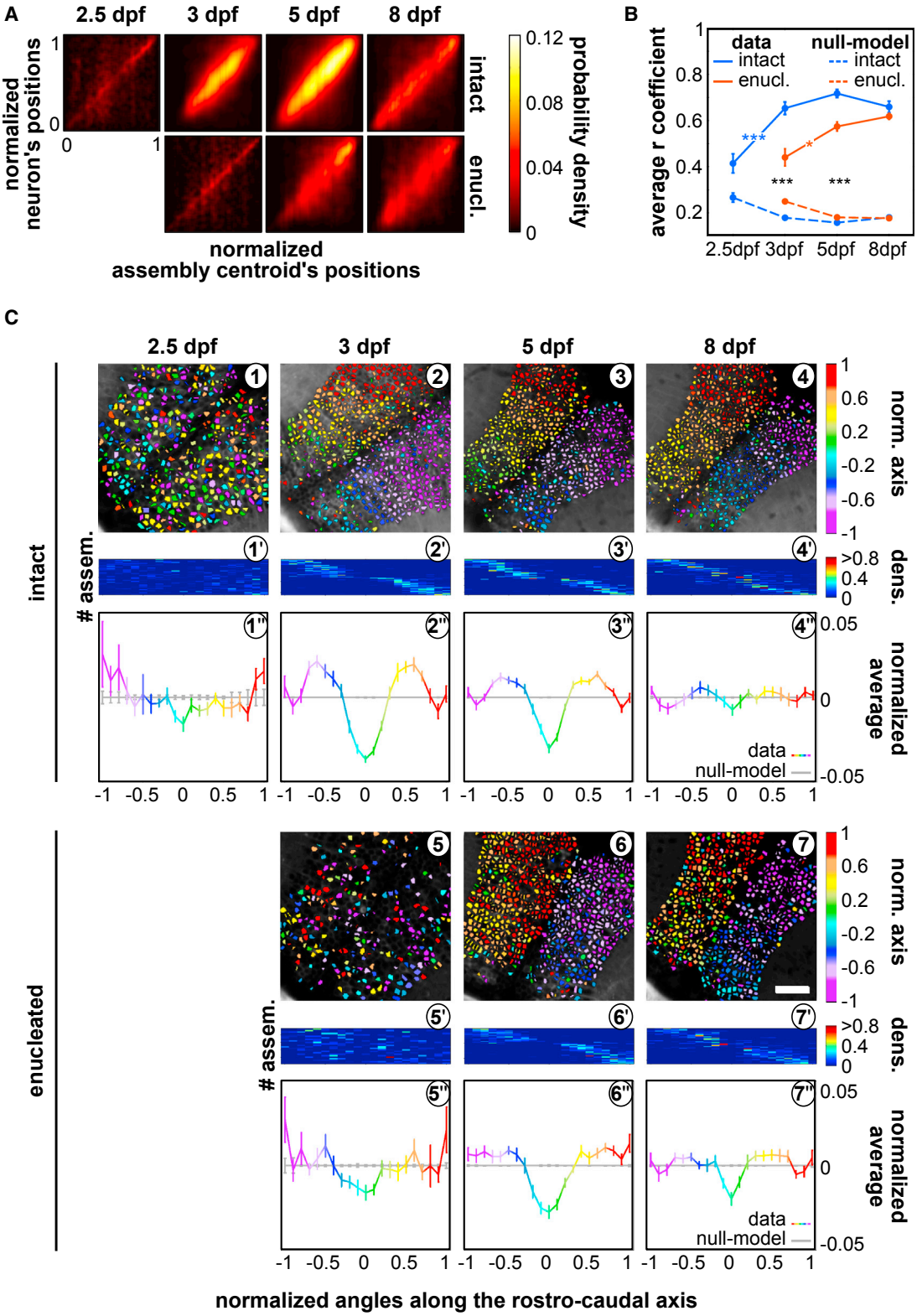

(legend on next page)

between the pattern of active neurons at each imaged frame, with respect to the neurons belonging to a given assembly. It ranges from 0 to 1, where 1 represents a full match between the topography of a given assembly and that of the imaged activity pattern, and 0 represents a complete mismatch. Using this index, we analyzed the temporal dynamics of each neuronal assembly. Each assembly was active several times during the recording period, and their frequency increased significantly throughout development in both intact and enucleated larvae (Figure S2D).

In the functionally mature optic tectum (8 dpf), the spontaneous neuronal assemblies grouped neurons with similar selectivities for spatial positions of the visual field (similar spatial tuning curves) and resembled neuronal response patterns induced by spatially localized visual stimuli (Romano et al., 2015). To establish whether this property is already present at the onset of retinotectal connections, we measured the tectal neuronal responses to light spots of 20°, presented across the visual field of 3-dpf larvae, and compared them to those of 8-dpf larvae (Figures S3A and S3B). We observed that spontaneous assemblies tended to regroup neurons with similar spatial tuning curves (visual receptive fields) in both 3- and 8-dpf larvae (Figures S3C–S3E). These results indicate that the spontaneous neuronal assemblies regroup functionally related neurons already at the onset of retinotectal interactions, further suggesting that the formation of the functional assemblies is, most likely, independent of visual experience.

The tectum is a multisensory structure; its ventral layers receive inputs from the lateral line and the auditory system (Nevin et al., 2010). Therefore, it is possible that the spontaneous assemblies that we observed in the dorsal visual layers of the optic tectum could represent spontaneous activation of other sensory modalities. To control for this possibility, we stimulated the lateral line or the auditory system of zebrafish larvae, while monitoring tectal activity, in intact and enucleated 8-dpf larvae. We observed that these modalities were weakly represented in the ventral part of the tectum of intact larvae, and mostly absent in the dorsal visual layers, in both intact and enucleated larvae (Figures S3F–S3H). These results indicate that the chronic absence of retinal inputs did not generate plastic changes, leading to an increase of the auditory and the lateral line responses in the dorsal visual layers of the optic tectum. We thus suggest that the spatial structure of the ongoing tectal activity, capable of emerging in the absence of retinal inputs, represents the functional connectivity of the tectum associated with its visual role, rather than reflecting other non-visual sensory maps.

Overall, these results suggest that the ongoing spontaneous tectal activity is organized according to functional neuronal assemblies that, during development, become more compact and specific to a single tectal hemisphere. The absence of retinal inputs delayed the maturation of the neuronal assemblies but did not prevent it. In addition, at 8 dpf, intact larvae showed a slight decrease in the compactness and lateralization indices of the assemblies, supporting the idea of the possible emergence of new, extra tectal afferents or intertectal connectivity after 5 dpf.

Spontaneous Neuronal Assemblies Reveal a Tectal Topographic Organization

It was previously shown in the functionally mature network that the spontaneous neuronal assemblies reflect the retinotopic map of the optic tectum (Romano et al., 2015). We asked whether a spatial organization of the tectal spontaneous activity is present even before functional retinotectal interactions, how it changes during maturation, and how it is affected by the chronic deprivation of all retinal inputs. We first determined which tectal morphological axes best described the topographic organization of the neuronal assemblies, according to our imaging plane. We calculated the correlation coefficient (r) of the linear regression between the position of the centroid of each assembly and the position of each of the neurons within the assembly in a common spatial reference (Figure S4A; Niell and Smith, 2005). A strong correlation would indicate that the assemblies are composed of neighboring neurons rather than showing sparse topographies. The axis with the highest r values best fitted the caudo-rostral axis for all developmental stages for both intact and enucleated larvae (Figure S4B). Therefore, we used the average r coefficients along this axis as a measure of the global topographic organization level of tectal spontaneous assemblies and compared them to those of the respective null-models to assess their significance (Figures 3A, 3B, and S4C). Despite the absence of significant temporal correlations, intact larvae showed weak, although significant, topographic organization already at 2.5 dpf ($p < 0.004$ when compared to 2.5-dpf null models), suggesting that a spontaneous activity spatial structure is already present before the retina functionally

Figure 3. The Spontaneous Neuronal Assemblies Progressively Organize along the Tectal Caudo-rostral Axis, during Development

(A) Density plots of the caudo-rostral normalized positions of each neuron against the normalized position of each neuronal assembly centroid along the caudo-rostral axis of the tectum, in intact and enucleated (enucl.) larvae, at each developmental stage; 0 is the most rostral position and 1 is the most caudal one (in the enucleated 8-dpf larva density plot; the respective null models are in Figure S4C).

(B) Average r coefficients of the regression fit between the position of the assembly's centroids and that of the assembly's neurons, along the caudo-rostral axis, in intact (blue) and enucleated (enucl.; red) larvae. The respective null models are depicted by the dashed curves in the right panel. ***$p < 0.001$.

(C) Topographic organization of the spontaneous neuronal assemblies. (1–4) Examples of assemblies' topographies projected along the caudo-rostral axis of an intact larva at different developmental stages. Color bar: position along the caudo-rostral axis (the neurons are color coded according to the centroid azimuthal position of the assembly to which they belong). (5–7) Same as for (1)–(4), but for the enucleated larvae. Scale bar represents 100 μm. (1'–7') Distribution of the density of number of neurons belonging to each assembly, along the normalized (norm.) caudo-rostral axis, for the experiment illustrated in (1)–(7), respectively; y axis: neuronal assembly number (# assem.); x axis: normalized caudo-rostral tectal axis (see Figure S4D for the distributions of all experiments and their respective null models). Color bar: neuronal density along the normalized caudo-rostral axis (dens.). (1''–7'') Average normalized mean distributions of the assemblies' neuronal densities in (1')–(7'), for all experiments during the different developmental stages, in intact and enucleated conditions, color coded accordingly to their normalized azimuthal positions (color bar). The normalized mean distributions of the respective null models are depicted in gray.

Error bars indicate SEM. See also Figure S4.

connects to the tectum and highlighting the early role of molecular cues in the topographic organization of the tectal circuitry. At 3 dpf, this spatial organization significantly strengthened with the arrival of the retinal inputs ($p < 10^{-4}$) and did not significantly change subsequently (3 versus 5 or 8 dpf and 5 versus 8 dpf: $p > 0.14$). In enucleated larvae, the average r coefficient at 3 dpf was not significantly different from that of 2.5-dpf intact larvae ($p > 0.85$), yet it reached values similar to those of intact larvae at 8 dpf ($p > 0.18$).

To estimate how well the different regions of the optic tectum are represented by the spontaneous neuronal assemblies, we calculated the density of neurons within an assembly along the caudo-rostral axis (Figures 3C and S4D). Similar average density values would imply a homogeneous topographic organization where all regions of the larva's field of view are similarly represented by the spontaneous neuronal assemblies. To control for the increasing number of tectal neurons during development, we normalized the density distributions with respect to the null models (Figures 3C1''–3C7'').

Already at 2.5 dpf, the caudal domains of the optic tectum contained assemblies that were topographically denser than in the more frontal regions. This bias was further pronounced at 3 dpf, but it began to recede at 5 dpf and mostly disappeared at 8 dpf (the majority of the regions along the caudo-rostral axis presented a homogeneous distribution of densities, except for the most rostral position; $p = 0.034$; Figures 3C1''–3C4''). Enucleated larvae showed comparable developmental dynamics of average density values, although less pronounced and delayed. The 3-dpf enucleated larvae were similar to the 2.5-dpf intact ones ($p > 0.45$). At 8 dpf, the neuronal density of the assemblies along the caudo-rostral axis was more uniform and matched the topographic representation of intact larvae at the same developmental stage, except for the most rostral position ($p < 0.003$; Figures 3C5''–3C7'').

Overall, these results show that the tectal spontaneous activity has a topographical structure organized along the relevant functional retinotopic axis (Niell and Smith, 2005), which evolves over the course of development to reach a near-uniform distribution of the neuronal assemblies along this axis. The absence of retinal inputs delays, but does not prevent, the development of the spatial structure of the tectal spontaneous activity.

The Spontaneous Neuronal Assemblies Are Functional even in the Chronic Absence of Retinal Inputs

To assess whether the spontaneous assemblies remain functional even in the chronic absence of retinal inputs, we investigated their capacity to predict self-generated motor behaviors (Romano et al., 2015) at a developmental stage at which the optic tectum is functionally mature (8 dpf). Thus, we simultaneously monitored tectal spontaneous neuronal activity and spontaneous tail movements in intact and enucleated larvae (Figures 4A and 4B). In both conditions, larvae produced brief episodes of tail movements of equivalent duration (387 ms ± 32 ms and 388 ms ± 42 ms, respectively, for intact and enucleated larvae), but with a significantly higher frequency in the enucleated larvae (126–158 movements.hr^{-1} versus 59–75 movements.hr^{-1} in intact larvae; 95% confidence interval after a Jack-Knife procedure [$CI_{95\%}$]).

To assess the role of the spontaneous assemblies in predicting self-generated behaviors, we considered only tail movements separated by at least 5 s. In this manner, we ensured that the analyzed tectal activity was directly related to the succeeding movement rather than representing activity associated with the previous one. We observed that topologically compact groups of neurons (compactness index: 0.38 ± 0.04 in intact and 0.31 ± 0.02 in enucleated larvae) were activated just before the onset of the tail movements at a rate of 5.0 episodes.hr^{-1} in intact larvae and 4.8 episodes.hr^{-1} in enucleated larvae. Thus, we computed the chance of observing a self-generated movement, given the spontaneous activation of a tectal compact assembly before the movement. More precisely, we calculated the probability of generating a spontaneous tail movement as a function of the correlation between the patterns of tectal activity preceding the onset of a tail flip and the topographies of all the spontaneous neuronal assemblies found. This correlation indicates the degree of similarity between the activity of the tectal circuit preceding a movement and the topographies of the spontaneous compact neuronal assemblies (Figure 4C). We found that this probability sharply increased as the spontaneous tectal activity gradually matched the topography of the spontaneous assemblies. Surprisingly, the tail movement probability as a function of this correlation was not significantly different in intact and enucleated larvae (mostly overlapping $CI_{95\%}$; Figure 4C). These results indicate that the observed tectal spontaneous assemblies capable of emerging in the chronic absence of visual inputs are still functionally relevant with respect to its motor output.

DISCUSSION

Our results show that, before the formation of functional retinotectal connections, the spontaneous activity of the optic tectum displays characteristics reminiscent of nascent networks, largely composed of neurons in an immature state (Gu et al., 1994; Sheroziya et al., 2009), and weakly interconnected circuits. Right after the onset of retinotectal interactions (at 3 dpf, via excitatory glutamatergic inputs), we measured rapid changes in the network, likely due to the maturation of the different neuronal sub-populations of the tectal network (Sin et al., 2002). This hypothesis is in line with the observed delay in the emergence of the spatiotemporal structure of the spontaneous activity in enucleated larvae. In addition to activity-dependent mechanisms, it is also possible that molecular cues could play a role in the development of the tectum's ongoing spontaneous activity (e.g., secreted factors or cell-adhesion molecules that could be expressed by the RGCs; Triplett, 2014). By 8 dpf, the amplitude, frequency, and synchronization of Ca^{2+} events in enucleated larvae significantly increased above normal values. The early removal of retinal inputs have, therefore, a long-standing effect on the maturation of the tectal neurons reflected by an apparent increase in excitability (Akerman and Cline, 2006; Sernagor et al., 2003).

In addition, we showed that tectal spontaneous activity is significantly correlated at the single-cell level and organized in coherent neuronal assemblies that regroup neurons with similar functional properties and are arranged along the retinotopic tectal axis from the onset of the retinotectal functional

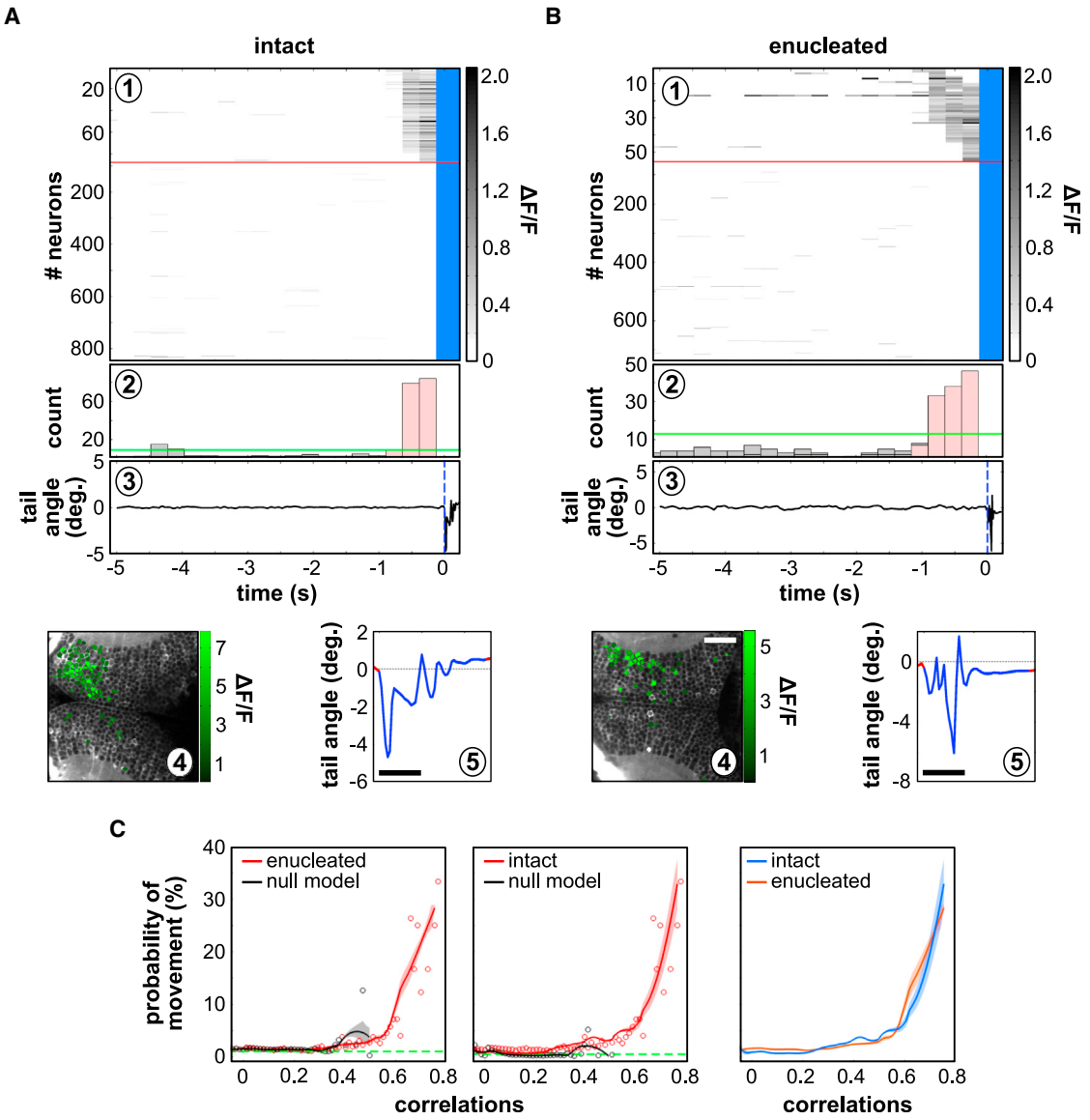

Figure 4. Spontaneous Neuronal Assemblies Are Predictive of Tail Motor Behaviors, even in Chronic Absence of Retinal Inputs

(A and B) Examples of spontaneous activation of a topographically compact tectal assembly before the onset of a tail movement in an intact larva (A) and an enucleated larva (B). (A1 and B1) Raster plot of all imaged tectal neurons; the red line separates the neurons belonging to the active neuronal pattern before the tail flip (above), from the rest of the neurons in the circuit (below; notice that the scale is different above and below the line; blue indicates frames during tail-flip movements). (A2 and B2) Histogram of the number of active neurons in the circuit; the fraction of neurons in the active neuronal pattern is represented in pink; the green line represents the threshold for significant neuronal population events. (A3 and B3) Tail angle. The blue dashed line indicates the onset of tail movement. Deg, degree. (A4 and B4) Topography of the spontaneously active neuronal pattern; compactness index: 0.54 (A4) and 0.33 (B4). (A5 and B5) A magnification of the angle of the tail during the movement. Scale bars, 100 ms.

(C) Probability of a tail movement as a function of the correlation between all assembly patterns and the spontaneous tectal network activity for the imaging frame preceding the movement onset in intact larvae (left; n = 6) and enucleated larvae (middle; n = 6). Red dots indicate raw data; black dots indicate null models; red curves indicate regression fits, with $CI_{95\%}$; black curves indicate null-model assemblies; and dashed green lines indicate global average probability of movements. Right: comparison between intact larvae (blue) and enucleated larvae (red).

connections (see also Romano et al., 2015). In the chronic absence of retinal inputs, the maturation of the spatial structure of the spontaneous activity was delayed with respect to intact larvae. However by 8 dpf, the topographic organization in intact and enucleated larvae became almost indistinguishable, strengthening the idea that neither visual experience nor the retinal patterned spontaneous activity is essential for the establishment of a proper topographic arrangement along the retinotopic axis of the optic tectum. The generation and maintenance of the spatial structure of the spontaneous activity is, thus, likely

determined by an intrinsic mechanism that organizes the circuit architecture of the optic tectum. The fact that the retina promotes the development of the spatial structure of the tectal spontaneous activity at an early stage of the development of the visual system, but is not essential for its further maturation, leads us to hypothesize that the predetermined tectal connectivity is strengthened by the level of retinal drive per se, rather than its patterned sensory inputs.

In the intact mature visual system of zebrafish larvae, the spontaneous activity spatial structure reflects the functional retinotopic tectal map and it is predictive of tail motor movements (see also Romano et al., 2015). We found that the predictive nature of the spontaneous activity in the mature tectum of enucleated larvae was similar to those of intact ones. This implies that, even in the chronic absence of retinal inputs, the tectal network is capable of connecting properly and projecting to its extratectal post-synaptic targets, suggesting that primary sensory inputs to the tectum are dispensable for the development of a functional tectal network.

Conclusions

We have shown that the retina strongly influences the development of the intrinsic connectivity of the optic tectum. However, the absence of visual inputs does not prevent a spatial organization of the spontaneous tectal activity that reveals neuronal assemblies associated with visuomotor transformations, supporting the idea that the tectal network is prone for its functional role. This capability may be an advantageous developmental strategy for the prompt execution of vital behaviors, such as escaping predators or catching prey, without requiring prior visual experience. However, this does not preclude the possibility that visual experience plays a role in the further refinement of the tectal circuitry.

EXPERIMENTAL PROCEDURES

Animals

Zebrafish were maintained on a 14-hr/10-hr light/dark cycle at a temperature of 28.5°C. HuC:GCaMP3^{ens100Tg} zebrafish larvae (Panier et al., 2013) in a Nacre background (mitfa$^{-/-}$) were raised up to 8 dpf, in 0.5× E3 embryo medium (Westerfield, 1995) and fed with paramecia after 5 dpf. All experiments were approved by Le Comité d'Éthique pour l'Expérimentation Animale Charles Darwin (03839.03).

In Vivo Imaging

To monitor the neuronal activity, we used a custom-built two-photon scanning microscope based on a MOM (Movable Objective Microscope) system (Sutter Instruments), with a 25×, NA 1.05 objective (Olympus) and a Mai-Tai DeepSee Ti:sapphire laser (Spectra-Physics) tuned to 920 nm. Collection of the emission light path consisted of FF705 dichroic, FF01-680 short-pass, and FF01 520/70 band-pass filters (Semrock). The photomultiplier tube was an H1070 (GaAsP; Hamamatsu). Its output signal was amplified with an SR-570 low-noise current preamplifier (Stanford Research Systems). The output excitation laser power at the focal plane was less than 3 mW. For data acquisition and controlling the galvanometers, we used ScanImage r3.8 (Pologruto et al., 2003). Data were acquired at ~3.91 Hz, with a resolution of 256 × 256 pixels (~0.262-mm^2 optical plane).

Data Analysis

Image segmentation to obtain regions of interest corresponding to neurons, curation of movement artifacts, and detection of the significant calcium transients were performed as described in Romano et al. (2015), using custom-written MATLAB scripts (MathWorks). Frames with movement artifacts were not further considered, and the non-significant portions of the ΔF/F traces were then set to 0 in all subsequent analysis.

All data were processed using custom-made scripts written in MATLAB. The Kolmogorov-Smirnov test was used for all statistical analyses, unless otherwise noted. In some cases, Wilcoxon signed-rank tests were used when comparisons with zero median were required. For comparisons between groups, we used the Jack-Knife procedure. This procedure is a non-parametric re-sampling method. Each observation is successively left out from a given dataset of n samples before estimating the mean of this sub-dataset. This procedure generates an $n - 1$ number of estimates. The average and variance of all these estimates are then calculated, and the 95% confidence interval is approximated (twice the squared root of the variance divided by n). All measured values were expressed as mean ± SEM. The levels of significance of the comparison between two conditions are: *$p < 0.05$; **$p < 0.01$; and ***$p < 0.001$.

SUPPLEMENTAL INFORMATION

Supplemental Information includes Supplemental Experimental Procedures and four figures and can be found with this article online at http://dx.doi.org/10.1016/j.celrep.2017.04.015.

AUTHOR CONTRIBUTIONS

Conceived and designed the experiments: T.P. and G.S. Performed the experiments: T.P., and J.B.-W. and V.C. for controls. Analyzed the data: T.P. Contributed reagents/materials/analysis tools: T.P., S.A.R., and V.P.-S. Wrote the paper: T.P. and G.S.

ACKNOWLEDGMENTS

The authors thank the members of the lab for their support and discussions, A. Jouary for help with tail movements' analysis, B. Barbour for comments on the manuscript, P. Gongal for editorial assistance, and F. Bouallage for the constant care of zebrafish. This work was supported by ERC stg 243106 (to G.S.), the Fondation pour la Recherche Médicale (to T.P.), ANR-10-LABX-54 (MEMO LIFE), and ANR-11-IDEX-0001-02 (PSL* Research University).

Received: June 14, 2016
Revised: February 15, 2017
Accepted: April 4, 2017
Published: May 2, 2017

REFERENCES

Ackman, J.B., and Crair, M.C. (2014). Role of emergent neural activity in visual map development. Curr. Opin. Neurobiol. *24*, 166–175.

Akerman, C.J., and Cline, H.T. (2006). Depolarizing GABAergic conductances regulate the balance of excitation to inhibition in the developing retinotectal circuit in vivo. J. Neurosci. *26*, 5117–5130.

Burbridge, T.J., Xu, H.-P., Ackman, J.B., Ge, X., Zhang, Y., Ye, M.-J., Zhou, Z.J., Xu, J., Contractor, A., and Crair, M.C. (2014). Visual circuit development requires patterned activity mediated by retinal acetylcholine receptors. Neuron *84*, 1049–1064.

Burrill, J.D., and Easter, S.S., Jr. (1994). Development of the retinofugal projections in the embryonic and larval zebrafish (Brachydanio rerio). J. Comp. Neurol. *346*, 583–600.

Faisal, A.A., Selen, L.P.J., and Wolpert, D.M. (2008). Noise in the nervous system. Nat. Rev. Neurosci. *9*, 292–303.

Fiser, J., Chiu, C., and Weliky, M. (2004). Small modulation of ongoing cortical dynamics by sensory input during natural vision. Nature *431*, 573–578.

Gahtan, E., Tanger, P., and Baier, H. (2005). Visual prey capture in larval zebrafish is controlled by identified reticulospinal neurons downstream of the tectum. J. Neurosci. *25*, 9294–9303.

Gu, X., Olson, E.C., and Spitzer, N.C. (1994). Spontaneous neuronal calcium spikes and waves during early differentiation. J. Neurosci. *14*, 6325–6335.

Huberman, A.D., Feller, M.B., and Chapman, B. (2008). Mechanisms underlying development of visual maps and receptive fields. Annu. Rev. Neurosci. *31*, 479–509.

Jetti, S.K., Vendrell-Llopis, N., and Yaksi, E. (2014). Spontaneous activity governs olfactory representations in spatially organized habenular microcircuits. Curr. Biol. *24*, 434–439.

Keck, T., Keller, G.B., Jacobsen, R.I., Eysel, U.T., Bonhoeffer, T., and Hübener, M. (2013). Synaptic scaling and homeostatic plasticity in the mouse visual cortex in vivo. Neuron *80*, 327–334.

Kenet, T., Bibitchkov, D., Tsodyks, M., Grinvald, A., and Arieli, A. (2003). Spontaneously emerging cortical representations of visual attributes. Nature *425*, 954–956.

Kirkby, L.A., Sack, G.S., Firl, A., and Feller, M.B. (2013). A role for correlated spontaneous activity in the assembly of neural circuits. Neuron *80*, 1129–1144.

Kita, E.M., Scott, E.K., and Goodhill, G.J. (2015). Topographic wiring of the retinotectal connection in zebrafish. Dev. Neurobiol. *75*, 542–556.

Krauzlis, R.J., Lovejoy, L.P., and Zénon, A. (2013). Superior colliculus and visual spatial attention. Annu. Rev. Neurosci. *36*, 165–182.

Nevin, L.M., Robles, E., Baier, H., and Scott, E.K. (2010). Focusing on optic tectum circuitry through the lens of genetics. BMC Biol. *8*, 126.

Niell, C.M., and Smith, S.J. (2005). Functional imaging reveals rapid development of visual response properties in the zebrafish tectum. Neuron *45*, 941–951.

Panier, T., Romano, S.A., Olive, R., Pietri, T., Sumbre, G., Candelier, R., and Debrégeas, G. (2013). Fast functional imaging of multiple brain regions in intact zebrafish larvae using selective plane illumination microscopy. Front. Neural Circuits *7*, 65.

Pologruto, T.A., Sabatini, B.L., and Svoboda, K. (2003). ScanImage: flexible software for operating laser scanning microscopes. Biomed. Eng. Online *2*, 13.

Pratt, K.G., Dong, W., and Aizenman, C.D. (2008). Development and spike timing-dependent plasticity of recurrent excitation in the Xenopus optic tectum. Nat. Neurosci. *11*, 467–475.

Romano, S.A.A., Pietri, T., Pérez-Schuster, V., Jouary, A., Haudrechy, M., and Sumbre, G. (2015). Spontaneous neuronal network dynamics reveal circuit's functional adaptations for behavior. Neuron *85*, 1070–1085.

Sernagor, E., Young, C., and Eglen, S.J. (2003). Developmental modulation of retinal wave dynamics: shedding light on the GABA saga. J. Neurosci. *23*, 7621–7629.

Sheroziya, M.G., von Bohlen Und Halbach, O., Unsicker, K., and Egorov, A.V. (2009). Spontaneous bursting activity in the developing entorhinal cortex. J. Neurosci. *29*, 12131–12144.

Sin, W.C., Haas, K., Ruthazer, E.S., and Cline, H.T. (2002). Dendrite growth increased by visual activity requires NMDA receptor and Rho GTPases. Nature *419*, 475–480.

Smith, M.A., and Kohn, A. (2008). Spatial and temporal scales of neuronal correlation in primary visual cortex. J. Neurosci. *28*, 12591–12603.

Stuermer, C.A. (1988). Retinotopic organization of the developing retinotectal projection in the zebrafish embryo. J. Neurosci. *8*, 4513–4530.

Sumbre, G., Muto, A., Baier, H., and Poo, M.M. (2008). Entrained rhythmic activities of neuronal ensembles as perceptual memory of time interval. Nature *456*, 102–106.

Tian, L., Hires, S.A., Mao, T., Huber, D., Chiappe, M.E., Chalasani, S.H., Petreanu, L., Akerboom, J., McKinney, S.A., Schreiter, E.R., et al. (2009). Imaging neural activity in worms, flies and mice with improved GCaMP calcium indicators. Nat. Methods *6*, 875–881.

Tolhurst, D.J., Movshon, J.A., and Dean, A.F. (1983). The statistical reliability of signals in single neurons in cat and monkey visual cortex. Vision Res. *23*, 775–785.

Triplett, J.W. (2014). Molecular guidance of retinotopic map development in the midbrain. Curr. Opin. Neurobiol. *24*, 7–12.

Vislay-Meltzer, R.L., Kampff, A.R., and Engert, F. (2006). Spatiotemporal specificity of neuronal activity directs the modification of receptive fields in the developing retinotectal system. Neuron *50*, 101–114.

Warp, E., Agarwal, G., Wyart, C., Friedmann, D., Oldfield, C.S., Conner, A., Del Bene, F., Arrenberg, A.B., Baier, H., and Isacoff, E.Y. (2012). Emergence of patterned activity in the developing zebrafish spinal cord. Curr. Biol. *22*, 93–102.

Weliky, M., and Katz, L.C. (1999). Correlational structure of spontaneous neuronal activity in the developing lateral geniculate nucleus in vivo. Science *285*, 599–604.

Westerfield, M. (1995). The Zebrafish Book: A Guide for the Laboratory Use of Zebrafish (Danio rerio) (University of Oregon Press).

Xu, H., Khakhalin, A.S., Nurmikko, A.V., and Aizenman, C.D. (2011). Visual experience-dependent maturation of correlated neuronal activity patterns in a developing visual system. J. Neurosci. *31*, 8025–8036.

Zhou, Q., Tao, H.W., and Poo, M.M. (2003). Reversal and stabilization of synaptic modifications in a developing visual system. Science *300*, 1953–1957.